

Column III-column V sublattice interaction via Zn and Si impurity-induced layer disordering of ^{13}C -doped $\text{Al}_x\text{Ga}_{1-x}\text{As}$ -GaAs superlattices

L. J. Guido,^{a)} J. S. Major, Jr.,^{b)} J. E. Baker, N. Holonyak, Jr., B. T. Cunningham, and G. E. Stillman

Electrical Engineering Research Laboratory, Center for Compound Semiconductor Microelectronics, and Materials Research Laboratory, University of Illinois at Urbana-Champaign, Urbana, Illinois 61801

(Received 4 October 1989; accepted for publication 27 November 1989)

Experiments are described employing secondary-ion mass spectroscopy (SIMS) to study the stability of ^{13}C -doped $\text{Al}_{0.5}\text{Ga}_{0.5}\text{As}$ -GaAs superlattices against Zn and Si impurity-induced layer disordering (IILD). The modulation depth of the SIMS ^{27}Al and ^{13}C signals is used as a sensitive probe of column III and column V sublattice interdiffusion. The data show that C_{As} is much more stable against Zn and Si IILD than the column III superlattice host crystal itself. The minor enhancement of C_{As} diffusion via the column III disordering agents, which is present to a significant extent for Si IILD but almost nonexistent for Zn IILD, suggests that there is no direct interchange of column III and column V sublattice atoms. The Zn and Si enhancement of carbon diffusion is probably caused by local Coulombic interaction between the diffusing Zn_i^+ and Si_{III}^+ species and the C_{As}^- acceptor.

Previous reports of optimized metalorganic chemical vapor deposition (MOCVD) for the growth of high-performance carbon-doped $\text{Al}_x\text{Ga}_{1-x}\text{As}$ -GaAs quantum well heterostructure (QWH) lasers,¹ and for similar QWHs doped via an independently controllable carbon doping source (CCl_4)² show that the As sublattice acceptor carbon (C_{As}) is perhaps one of the better *p*-type dopants for device use. These results are of interest not simply because carbon can be added to the existing selection of *p*-type dopants, but more importantly because carbon exhibits characteristics of an ideal dopant (see Refs. 1–3).

Earlier work on GaAs epitaxial crystals with $\sim 1000 \text{ \AA}$ ^{12}C doping spikes has demonstrated that during post-growth thermal annealing carbon diffusion is very slow, and is relatively independent of the surface encapsulant and the annealing ambient.³ Subsequent layer disordering experiments on ^{12}C -doped $\text{Al}_x\text{Ga}_{1-x}\text{As}$ -GaAs QWH crystals have shown that such heterostructures are even more stable against high-temperature annealing than the corresponding undoped QWH crystals.⁴ These results suggest that the C_{As} impurity influences Al-Ga interdiffusion on the column III sublattice. In the work described here, we use secondary-ion mass spectroscopy (SIMS) to explore the high-temperature stability of ^{13}C -doped $\text{Al}_{0.5}\text{Ga}_{0.5}\text{As}$ -GaAs superlattices (SL) with ^{13}C doping either in the barriers or in the wells. These QWH crystals are particularly suited for study of the column III-column V interaction, because diffusion on the As sublattice can be tracked via the SIMS ^{13}C signal without introducing an additional strain energy variable. The data show that ^{13}C doping spikes are more stable against Zn or Si impurity-induced layer disordering (IILD) than the superlattice host crystal itself. However, there is a significant interaction between the column III disordering agents, Zn and Si, and the As sublattice.

The QWH crystals used in this work have been grown by MOCVD in an Emcore GS3000-DFM reactor using the precursors trimethylgallium [$(\text{CH}_3)_3\text{Ga}$], trimethylaluminum [$(\text{CH}_3)_3\text{Al}$], and arsine (100%). The carbon doping source is 99% ^{13}C enriched carbon tetrachloride ($^{13}\text{CCl}_4$) diluted to 500 ppm in ultra-high purity H_2 . The ^{13}C isotope has been used to differentiate intentional carbon doping from the considerable ^{12}C background that exists in MOCVD-grown $\text{Al}_x\text{Ga}_{1-x}\text{As}$.⁵ The MOCVD growth conditions are a growth rate of $\sim 500 \text{ \AA min}^{-1}$, AsH_3 flow $\sim 100 \text{ sccm}$, total H_2 flow $\sim 9 \text{ slm}$, $T_G \sim 650 \text{ }^\circ\text{C}$, $p_G \sim 100 \text{ Torr}$, and a substrate rotation rate of $\sim 1500 \text{ rpm}$. The $^{13}\text{CCl}_4$ flow is fixed at $\sim 100 \text{ sccm}$ for each ^{13}C -doped layer, resulting in a hole concentration of $p_C \sim 10^{18} \text{ cm}^{-3}$. The basic QWH crystal consists of an undoped $\sim 2500 \text{ \AA}$ GaAs buffer layer grown on a Si-doped (100) GaAs substrate, followed by a 100-period ^{13}C -doped $\text{Al}_{0.5}\text{Ga}_{0.5}\text{As}$ -GaAs SL ($L_z \approx L_B \sim 250 \text{ \AA}$). The SL is confined symmetrically on top and bottom by a pair of $\sim 2000 \text{ \AA}$ ^{13}C -doped layers of $\text{Al}_{0.5}\text{Ga}_{0.5}\text{As}$. The upper $\text{Al}_{0.5}\text{Ga}_{0.5}\text{As}$ confining layer is further capped by a $\sim 1000 \text{ \AA}$ layer of ^{13}C -doped GaAs. The two QWH crystals of interest here differ only in the SL doping; either the GaAs wells or the $\text{Al}_{0.5}\text{Ga}_{0.5}\text{As}$ barriers are ^{13}C doped.

The QWH crystals are prepared for thermal annealing by degreasing in organic solvents followed by *e*-beam deposition of $\sim 300 \text{ \AA}$ of elemental Si as a source layer for the Si IILD case. For high-temperature annealing, one sample with and one without a Si diffusion source layer are loaded into a quartz ampoule along with a piece of solid As ($\sim 15 \text{ mg}$). The ampoule is evacuated to 10^{-6} Torr and sealed to give a final volume of $\sim 3 \text{ cm}^3$. The two crystals are then annealed at $825 \text{ }^\circ\text{C}$ for 24 h. The sample preparation for Zn IILD is identical except that ZnAs_2 ($\sim 5 \text{ mg}$) is used to provide the Zn and the excess As overpressures, and the annealing temperature is $600 \text{ }^\circ\text{C}$ (3 h). After annealing the crystals are transferred to a high-vacuum SIMS chamber for analysis under identical vacuum conditions. The SIMS mea-

^{a)} Now at Yale University, Department of Electrical Engineering, Center for Microelectronic Materials, and Structures, Box 2157 Yale Station, New Haven, CT 06520.

^{b)} Intel Doctoral Fellow.

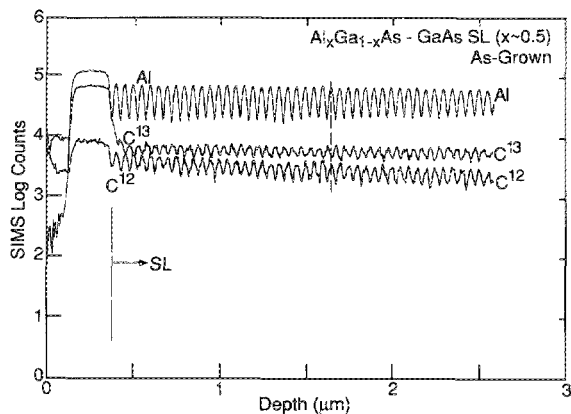


FIG. 1. Secondary-ion mass spectroscopy data for an as-grown $\text{Al}_x\text{Ga}_{1-x}\text{As}$ -GaAs SL with ^{13}C -doped GaAs wells ($L_z \sim 250 \text{ \AA}$). The ^{13}C signal is in phase with the ^{27}Al signal because of increased carbon incorporation during MOCVD growth of the $\text{Al}_{0.5}\text{Ga}_{0.5}\text{As}$ barriers (vertical dashed line). The ^{13}C signal is out of phase with the ^{27}Al signal because the $^{13}\text{CCl}_4$ source is turned on only during growth of the GaAs wells.

surement is performed using a Cameca IMS-3f ion probe with a Cs^+ primary ion source biased at +12.5 kV ($\sim 250 \text{ nA}$ beam current). The sample stage is biased at -4.5 kV for negative secondary-ion detection.

The SIMS data of Fig. 1 for the as-grown $\text{Al}_{0.5}\text{Ga}_{0.5}\text{As}$ -GaAs SL with ^{13}C -doped wells (and not barriers) show that intentional ^{13}C doping can be achieved independently of the MOCVD-related ^{12}C background. The large SIMS ^{12}C background signal is typical of MOCVD-grown $\text{Al}_x\text{Ga}_{1-x}\text{As}$ because carbon incorporation is a direct consequence of pyrolysis of the 98.9% ^{12}C -enriched metalorganic precursors $(\text{CH}_3)_3\text{Ga}$ and $(\text{CH}_3)_3\text{Al}$.⁵ For the study of $\text{Al}_x\text{Ga}_{1-x}\text{As}$ -GaAs heterostructures via SIMS depth profiling, the carbon background problem is amplified further by an increase in ^{12}C incorporation and in the SIMS carbon ion yield, with increasing Al mole fraction. These problems are exhibited in the ^{12}C depth profile of Fig. 1. The increase in the ^{12}C background signal is in phase with the increase in the ^{27}Al signal in the $\text{Al}_{0.5}\text{Ga}_{0.5}\text{As}$ barriers (vertical dashed line). In contrast, the intentional ^{13}C -doping signal is exactly 180° out of phase with the ^{27}Al signal, because the $^{13}\text{CCl}_4$ source is turned-on only during growth of the GaAs wells. The average ^{13}C signal in Fig. 1 is significantly larger than the average ^{12}C signal ($^{13}\text{C}/^{12}\text{C} \sim 2$). For comparison purposes, the SIMS $^{13}\text{C}/^{12}\text{C}$ ratio for an undoped SL crystal (data not shown) is ≤ 0.01 in accordance with the natural isotope abundance ratio ($^{13}\text{C}/^{12}\text{C} \sim 0.011$).

The SIMS data of Fig. 2 for an $\text{Al}_{0.5}\text{Ga}_{0.5}\text{As}$ -GaAs SL with ^{13}C -doped barriers (and not wells) demonstrate the high-temperature stability of both the SL heterointerfaces and the ^{13}C -doping spikes. The ^{27}Al signal modulation depth after crystal annealing at 825°C for 24 h (+15 mg As) is equal to the as-grown doped-GaAs SL crystal of Fig. 1. The ^{12}C signals of Figs. 1 and 2 are in good agreement, because the MOCVD growth parameters that affect ^{12}C background incorporation are identical. The ^{13}C depth profile of Fig. 2 exhibits a much larger average SIMS signal and depth of modulation than in Fig. 1 because of the higher carbon in-

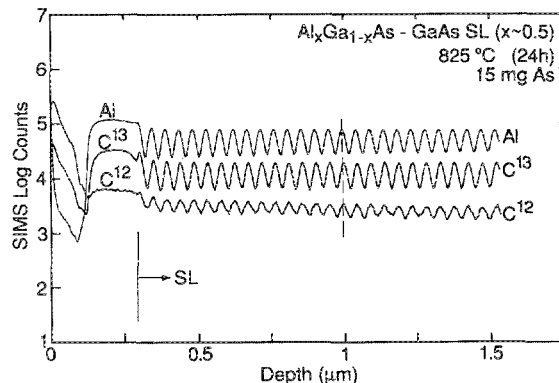


FIG. 2. Secondary-ion mass spectroscopy data for a ^{13}C -doped $\text{Al}_x\text{Ga}_{1-x}\text{As}$ -GaAs SL after annealing at 825°C for 24 h (+15 mg As). The superlattice differs from the crystal of Fig. 1 in that the $\text{Al}_{0.5}\text{Ga}_{0.5}\text{As}$ barriers are selectively doped with ^{13}C . The ^{27}Al , ^{13}C , and ^{12}C signals are in phase as indicated by the vertical dashed line, and the modulation depth for all three signals is unaffected by high-temperature annealing.

corporation and SIMS ion yield for the ^{13}C -doped $\text{Al}_{0.5}\text{Ga}_{0.5}\text{As}$ barriers. The key issue here is that the ^{13}C -doping spikes are at least as stable against high-temperature annealing as the $\text{Al}_{0.5}\text{Ga}_{0.5}\text{As}$ -GaAs SL heterointerfaces.

The SIMS data of Fig. 3 demonstrate that the ^{13}C -doping spikes are, in fact, more stable against Zn IILD than the SL host crystal itself. The low-temperature Zn diffusion (600°C , 3 h) has greatly enhanced Al-Ga interdiffusion at the barrier-well heterointerfaces as evidenced by the flat Al depth profile between ~ 0.25 and $1.25 \mu\text{m}$. The ^{27}Al signal modulation returns with a corresponding decrease in Zn concentration ($> 1.25 \mu\text{m}$). The intentional ^{13}C -doping spikes and the ^{12}C background spikes in the $\text{Al}_{0.5}\text{Ga}_{0.5}\text{As}$ barriers show only a slight decrease in modulation depth for the Zn-IILD crystal relative to the nondisordered SL layers. The two possible sources of the reduced SIMS carbon signal modulation are (1) an interaction between Zn diffusion on the column III sublattice and C diffusion on the column V sublattice, and (2) a change in SIMS carbon ion yield from the as-grown SL to the layer-averaged $\text{Al}_x\text{Ga}_{1-x}\text{As}$ crystal ($x \sim 0.25$).

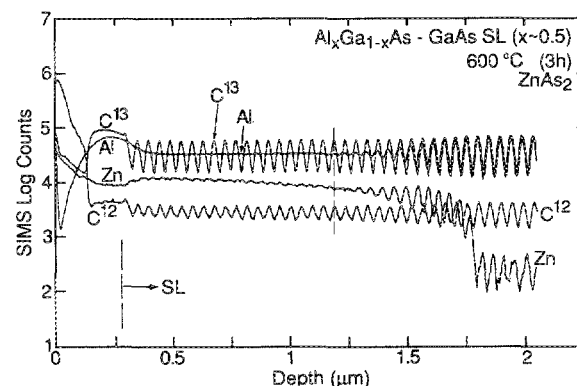


FIG. 3. Secondary-ion mass spectroscopy data for the SL of Fig. 2 after Zn diffusion at 600°C (3 h). The ^{13}C -doping spikes remain sharp despite complete Zn IILD of the superlattice host crystal (between ~ 0.25 and $1.25 \mu\text{m}$). Both carbon signals exhibit a slight reduction in modulation in the Zn IILD crystal.

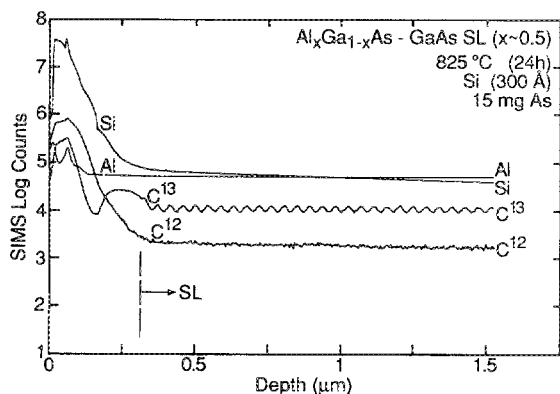


FIG. 4. Secondary-ion mass spectroscopy data for the SL of Fig. 2 after Si diffusion at 825 °C (24 h). The "flat" ^{27}Al signal results from Si diffusion and impurity-induced layer averaging of the heterointerfaces. Unlike for the SIMS data of Figs. 2 and 3 the modulation in carbon signals is almost completely eliminated by Si IILD.

Additional evidence of interaction between a column III disordering agent and the column V sublattice is given by the SIMS depth profile shown in Fig. 4. After Si diffusion at 825 °C for 24 h (+ 15 mg As) the SL crystal with ^{13}C -doped barriers exhibits a constant SIMS ^{27}Al signal characteristic of uniformly intermixed $\text{Al}_{0.5}\text{Ga}_{0.5}\text{As}$ barriers and GaAs wells. The SIMS measurement is discontinued before reaching the Si diffusion front as evidenced by the constant Si signal throughout the depth profile. The SIMS signal modulation for the Si IILD crystal is significantly reduced for ^{13}C and almost completely eliminated for ^{12}C in contrast to the Zn IILD data of Fig. 3. We emphasize that the annealing (only) data of Fig. 2 demonstrate that the reduced carbon modulation is not simply caused by the higher temperature used for the Si diffusion. These contrasting results lend support to the interpretation that the reduced SIMS carbon signal modulation is affected by Zn or Si IILD enhancement of carbon diffusion itself, and not simply by a change in SIMS ion yield.

There have been many reports of impurity-enhanced column III (Al, Ga, In) and column V (As, P) interdiffusion via Zn and Si IILD.⁶ In most cases, host atom interdiffusion is much greater on the column III sublattice than on the

column V sublattice.^{7,8} In the work described here we use C_{As} diffusion on the As sublattice as a sensitive (low concentration) probe of Zn and Si diffusion-enhanced column V interdiffusion. The data show that the C-doping spikes are much more stable against Zn and Si IILD than the column III SL host crystal itself, and that Si IILD enhances C_{As} diffusion to a much greater extent than does Zn IILD.⁷ We rule out any major contribution from indirect effects such as the Fermi level and electric field enhancement because the C diffusion trends observed here are contrary to earlier high-temperature annealing results for ^{12}C -doping spikes in p^+ - and n^+ -GaAs.³ The relatively minor diffusion enhancement exhibited by the low concentration C_{As} probe suggests that there is no direct interchange between column III and column V sublattice atoms during Zn and Si IILD. We propose that the high-temperature stability of C_{As} -doping spikes is related to the low diffusivity of carbon on the As sublattice, and that Zn and Si enhancement of carbon diffusion is caused by local Coulombic interaction between the diffusing Zn^{I} and $\text{Si}_{\text{III}}^{\text{II}}$ species and the C_{As} acceptor.

The authors are grateful to T. A. Richard for contributions to the experimental work, and to R. T. Gladin and B. L. Payne for assistance in manuscript preparation. This work has been supported by Army Research Office contract DAAL 03-89-K-0008 and the National Science Foundation grants CDR 85-22666 and DMR 86-12860.

¹L. J. Guido, G. S. Jackson, D. C. Hall, W. E. Plano, and N. Holonyak, Jr., *Appl. Phys. Lett.* **52**, 522 (1988).

²B. T. Cunningham, M. A. Haase, M. J. McCollum, and G. E. Stillman, *Appl. Phys. Lett.* **54**, 1905 (1989).

³B. T. Cunningham, L. J. Guido, J. E. Baker, J. S. Major, Jr., N. Holonyak, Jr., and G. E. Stillman, *Appl. Phys. Lett.* **55**, 687 (1989).

⁴L. J. Guido, B. T. Cunningham, D. W. Nam, K. C. Hsieh, W. E. Plano, J. S. Major, Jr., E. J. Vesely, A. R. Sugg, N. Holonyak, Jr., and G. E. Stillman, *J. Appl. Phys.* **67**, 15 Feb. (1990).

⁵T. F. Kuech, D. J. Colford, E. Veuhoff, V. Deline, P. M. Mooney, R. Potemski, and J. Bradley, *J. Appl. Phys.* **62**, 632 (1987).

⁶For a review, see D. G. Deppe and N. Holonyak, Jr., *J. Appl. Phys.* **64**, R93 (1988).

⁷S. A. Schwarz, P. Mai, T. Venkatesan, R. Bhat, D. M. Hwang, C. L. Schwartz, M. Koza, L. Nazar, and B. J. Skromme, *Appl. Phys. Lett.* **53**, 1051 (1988).

⁸H.-H. Park, B. K. Kang, E. S. Nam, Y. T. Lee, J. H. Kim, and O'D. Kwon, *Appl. Phys. Lett.* **55**, 1768 (1989).